

# Adaptive numerical designs for the calibration of computer models

Guillaume Damblin  
EDF R&D MRI, Chatou, France  
AgroParisTech / UMR INRA MIA  
INRA, UMR 518, F-75005 Paris, France

Pierre Barbillon\*<sup>†</sup>  
AgroParisTech / UMR INRA MIA  
INRA, UMR 518, F-75005 Paris, France

Merlin Keller  
EDF R&D MRI, Chatou, France

Alberto Pasanisi  
EDF R&D MRI, Chatou, France  
EIFER, Karlsruhe, Germany

Éric Parent  
AgroParisTech / UMR INRA MIA  
INRA, UMR 518, F-75005 Paris, France

June 17, 2022

## Abstract

Making good predictions about a physical system using a computer model requires the inputs to be carefully specified. Some of these inputs called control variables have to reproduce physical conditions whereas other inputs, called parameters, are specific to the computer model and most often uncertain. The goal of statistical calibration consists in tuning these parameters to make the outputs of the computer model as close as possible to the field measures. Where prior information is available, Bayesian inference can be conducted using MCMC methods, which are unfortunately unfeasible when the simulations are too time-consuming. A way to circumvent this issue is to emulate the computer model with a Gaussian process emulator. Using such a cheap approximation in the calibration process causes a new source of uncertainty which strongly depends on the choice of a numerical design of experiments from which this emulator is fitted. This uncertainty can be reduced by building a proper sequential design which is adapted to the calibration goal using the Expected Improvement criterion. Numerical illustrations in several dimensions are provided to assess the efficiency of such sequential strategies.

**Keywords:** Bayesian calibration, Gaussian process emulation, expected improvement criterion.

## 1 Introduction

This work is incorporated within the field of uncertainty quantification in computer experiments. A crucial issue in engineering (aerospace, car, nuclear, etc.) concerns the ability of computer models (also called simulators or computer codes) to mimic a physical phenomenon of interest

---

\*Corresponding author: 16 rue Claude Bernard, 75005 Paris

<sup>†</sup>PIERRE.BARBILLON@AGROPARISTECH.FR

as well as possible. In this regard, the field of so-called Verification and Validation (V&V) (Trucano et al., 2006; Roy and Oberkampf, 2011) aims at using statistical tools to assess the accuracy of computer predictions for many applications. For instance, the study of V&V has become a huge preoccupation in the nuclear industry where simulation is more and more used to assess the safety of installations for which physical experiments are impractical or economically unfeasible. An essential prerequisite of V&V consists in quantifying all sources of uncertainty involved in a computer experiment. In the paper, we focus on the uncertainty tainting some parameters of the model which are either non-measurable physical quantities or just tuning factors. After a statistical model has been assumed on the relationship between the computer model and the physical system, calibration (Campbell, 2006; Cox et al., 2001) comes down to a statistical inference of these parameters by minimizing the difference between the simulations and the available field data. Another popular framework which is quite different from calibration is named History Matching (HM) (Craig et al., 1997). Based on an implausibility measure, HM is well-suited for large systems for which the size of inputs makes immediate calibration intractable. HM aims at detecting regions of parameter space which appear to be incompatible with the field data. In the same way, Sensitivity Analysis (SA) (Saltelli et al., 2000) aims at detecting which parameters have negligible effect on the output of the model. Hence, these methods help shrink the input space before carrying out calibration.

Throughout the paper, our work focuses on Bayesian calibration (Bernardo and Smith, 1994; Parent and Bernier, 2007). This strategy of inference provides an appropriate framework to sequentially update the parametric variability from *prior* to *posterior* distribution as new data become available. Additionally, it can incorporate some expert knowledge to be encoded in the original *prior* distribution (Keller et al., 2011). We will suppose there exists a set of parameters making a perfect agreement between the field data and the model. In the literature, several papers deal with calibration in an extended framework where the model predictions suffer from a systematic discrepancy for any value of parameters (Kennedy and O’Hagan, 2001; Higdon et al., 2004). Even if this hypothesis seems more realistic due to the inability of a model to perfectly mimic the real world, it may induce some additional identifiability problems (Loeppky et al., 2006; Bayarri et al., 2007) that are out of the scope of this paper.

Our work rather focuses on the way to overcome two other critical issues frequently arising in calibration. On the one hand only a limited number of field data can be collected. On the other hand, simulations are often highly time-consuming. Indeed, it is quite frequent that a simulation needs several hours, even several days to run, thus making the MCMC algorithms impractical. A well-known solution to this issue is to replace the model in the likelihood expression by a Gaussian process emulator. A set of inputs from which the model is run is called numerical design of experiments and is required to fit this emulator. In the field of HM, subsequent waves of simulations are launched in order to refine the Gaussian process emulator. However, choosing the new inputs from which a new wave is run is still a challenging problem (Williamson and Vernon, 2015). In this paper, we propose a new algorithm for building sequential designs aiming at reducing the uncertainty which affects Bayesian calibration of costly computer models. To our knowledge, few papers deal with the impact of the design on the calibration uncertainty induced by a Gaussian process emulator. Kumar (2008) introduced some empirical criteria for sequentially selecting both computer and physical experiments to reduce the calibration error. Williams et al. (2011) dealt with sequential algorithms for adding physical experiments. Pratola et al. (2013) proposed some adaptive strategies whereby a criterion known as the EI (*Expected Improvement*) is computed over a likelihood ratio. This criterion is used to optimize black box models when a limited number of simulations is allocated (Jones et al., 1998). Besides that, this criterion has been applied to solving a problem of optimization under uncertainty when the

model inputs are  $(\mathbf{x}, \mathbf{u})$  where  $\mathbf{x}$  denotes a vector of control variables and  $\mathbf{u}$  denotes a vector of random variables (Janusevskis and Le Riche, 2013). In the same spirit, we propose new algorithms which consist in computing the EI criterion but applying it to the sum of squares of the residuals when the model inputs are  $(\mathbf{x}, \mathbf{t})$  where  $\mathbf{t}$  is a vector of parameters. In this way, we hope to reduce the uncertainty due to the Gaussian process emulator in regions of high *posterior* density.

This paper is divided into five sections. In Section 2, the statistical framework is introduced, then the main features of the Gaussian process emulator are recalled. In Section 3, two new algorithms for Bayesian calibration based on the Expected Improvement criterion are presented. Their performance is displayed on two academic examples in Section 4. The conclusions of this paper are provided in Section 5.

## 2 Calibration framework

**Notations and modeling** Let  $r(\mathbf{x}) \in \mathbb{R}$  be a physical system of interest where  $\mathbf{x} \in \mathcal{X} \subset \mathbb{R}^d$  is a vector of control variables. This kind of variable is measurable in the field and characterizes the system, including both physical variables (temperature, pressure, velocity, etc.) and design variables (height, area, etc.). We suppose in the paper that only a small number of field experiments, say  $n$ , has been collected. The matrix  $\mathbf{X}_f = [(\mathbf{x}_f^1)^T, \dots, (\mathbf{x}_f^n)^T]^T \in M_{n,d}(\mathbb{R})$  denotes the corresponding design of field experiments. Let  $\mathbf{z}_f = (\mathbf{z}_f^1, \dots, \mathbf{z}_f^n)$  be the vector of the  $n$  imprecise measures of  $r(\mathbf{X}_f) := (r(\mathbf{x}_f^1), \dots, r(\mathbf{x}_f^n))$ . For  $1 \leq i \leq n$ , we have

$$\mathbf{z}_f^i = r(\mathbf{x}_f^i) + \epsilon^i, \quad (1)$$

where

$$\epsilon^i \sim \mathcal{N}(0_n, \lambda^2 \mathbf{I}_n)$$

is a Gaussian white noise of variance  $\lambda^2$ .

Let  $y_{\mathbf{t}}(\mathbf{x})$  be a deterministic computer model which predicts  $r(\mathbf{x})$ . The vector  $\mathbf{t}$  is a vector of parameters including either factors attached to the field (chemical rate, friction coefficient, etc.) or mathematical factors having no counterpart in physics, or perhaps both. The computer model is seen as a black box function, which supposes nothing is known about the connection between the inputs  $(\mathbf{x}, \mathbf{t})$  and the output  $y_{\mathbf{t}}(\mathbf{x})$ . A simulation (or a computer experiment) is a model output  $y_{\mathbf{t}}(\mathbf{x})$  after the computer model is run. A set of input vectors from which the computer model is run is named a numerical design of experiments (Koehler and Owen, 1996). Following Kennedy and O’Hagan (2001), the computer model should be considered as an imperfect representation of the phenomenon  $r$ . Hence,

$$r(\mathbf{x}) = y_{\boldsymbol{\theta}}(\mathbf{x}) + b(\mathbf{x}), \quad (2)$$

where  $b(\mathbf{x})$  is the model discrepancy and  $\boldsymbol{\theta}$  is the optimal value of parameters. The statistical model is then given by

$$\mathbf{z}_f^i = y_{\boldsymbol{\theta}}(\mathbf{x}_f^i) + b(\mathbf{x}_f^i) + \epsilon^i. \quad (3)$$

The computer model is said to be calibrated when an estimator  $\hat{\boldsymbol{\theta}}$  of  $\boldsymbol{\theta}$  has been calculated as being the “best-fitting” parameter according to the statistical model (3). The estimation of  $\boldsymbol{\theta}$  in the model (3) requires us to set some *prior* hypothesis on the structure of  $b(\mathbf{x})$  to avoid intricate identifiability issues. This task has been discussed in several papers over the past decade (Kennedy and O’Hagan, 2001; Loepky et al., 2006; Bayarri et al., 2007). In this paper, we focus on the unbiased model where the model error is supposed to be negligible.

**The unbiased model** Let us suppose that  $b(\mathbf{x}) = 0$ . In other words, for at least one value  $t$  denoted by  $\theta \in \mathcal{T}$ , the computer model is supposed to be a perfect representation of the physical phenomenon  $r$ , which means that

$$\exists \theta \in \mathcal{T} ; \forall \mathbf{x} \in \mathcal{X}, r(\mathbf{x}) = y_{\theta}(\mathbf{x}). \quad (4)$$

Combining (4) and (1) leads to the equation

$$\mathbf{z}_{\mathbf{f}}^i = y_{\theta}(\mathbf{x}_{\mathbf{f}}^i) + \epsilon^i. \quad (5)$$

Such a model corresponds to an inverse problem since  $\theta$  is learned from the output (Barbillon et al., 2011). We have chosen to conduct a Bayesian inference of  $\theta$  because it has been shown to be better suited than the plug-in MLE for high dimensional calibration problems where the likelihood may be quite flat (Kumar, 2008). Let  $y_{\theta}(\mathbf{X}_{\mathbf{f}}) := (y_{\theta}(\mathbf{x}_{\mathbf{f}}^1), \dots, y_{\theta}(\mathbf{x}_{\mathbf{f}}^n))$  be the vector of model outputs running over the field data  $\mathbf{X}_{\mathbf{f}}$ . The *posterior* distribution of  $\theta$  comes from the Bayes formula:

$$\begin{aligned} \Pi(\theta|\mathbf{z}_{\mathbf{f}}) &\propto L(\mathbf{z}_{\mathbf{f}}|\theta)\Pi(\theta), \\ &\propto \frac{1}{(\sqrt{2\pi}\lambda)^n} \exp\left[-\frac{1}{2\lambda^2}SS(\theta)\right]\Pi(\theta), \end{aligned} \quad (6)$$

where

$$SS(\theta) = \|\mathbf{z}_{\mathbf{f}} - y_{\theta}(\mathbf{X}_{\mathbf{f}})\|^2 \quad (7)$$

is the Euclidean norm in  $\mathbb{R}^n$  of the sum of squares of the residuals. No closed-form formula exists for  $\Pi(\theta|\mathbf{z}_{\mathbf{f}})$  because  $y$  is usually highly non linear with respect to  $\theta$ . Samples from  $\Pi(\theta|\mathbf{z})$  can be collected running an MCMC (*Monte Carlo Markov Chain*) algorithm (Robert and Casella, 1998). Its convergence to the stationary state of the chain (here the distribution of interest  $\Pi(\theta|\mathbf{z})$ ) is only reached over a very large number of samples, often several thousand. In our framework, the MCMC algorithms are thus impractical since each sample requires a likelihood computation which itself depends on a time-consuming simulation. A way to tackle this problem consists in setting a Gaussian process  $Y$  as a *prior* distribution on  $y$ . Let us now provide some details about the Gaussian process emulator.

**Gaussian process emulator** This is used to encode a *prior* model structure on a deterministic computer model. Let  $\mathbf{D}_{\mathbf{N}} \in (\mathcal{X} \times \mathcal{T})^N$  be a numerical design of experiments:

$$\mathbf{D}_{\mathbf{N}} := \{(\mathbf{x}^1, \mathbf{t}^1), \dots, (\mathbf{x}^N, \mathbf{t}^N)\}. \quad (8)$$

After running the model over  $\mathbf{D}_{\mathbf{N}}$ ,  $N$  simulations can be collected:

$$\mathbf{y}(\mathbf{D}_{\mathbf{N}}) := \{y(\mathbf{x}^1, \mathbf{t}^1) := y_{\mathbf{t}^1}(\mathbf{x}^1), \dots, y(\mathbf{x}^N, \mathbf{t}^N) := y_{\mathbf{t}^N}(\mathbf{x}^N)\}. \quad (9)$$

For  $1 \leq i \leq N$ , the simulations are assumed as being sampled from a trajectory of a Gaussian process,

$$y(\mathbf{x}^i, \mathbf{t}^i) := y_{\mathbf{t}^i}(\mathbf{x}^i) \sim Y = \mathcal{P}\mathcal{G}(m_{\beta}(\cdot), \sigma^2 \Sigma_{\Psi}(\cdot)), \quad (10)$$

where

- $m_{\beta}(\cdot)$  is a mean vector (of size  $N \times 1$ ) where  $\beta$  is a vector of regression parameters,
- $\sigma^2$  the variance of the process,

- $\Sigma_{\Psi}$  is the correlation matrix of  $\mathbf{D}_{\mathbf{N}}$  (of size  $N \times N$ ) where  $\Psi$  is a vector of hyper-parameters including the correlation lengths and possibly a smoothness parameter.

The structure of  $\Sigma_{\Psi}$  depends on the choice of a kernel (Vazquez, 2005). For both practical and theoretical reasons, a stationary kernel is often set (Stein, 1999). The emulator (10) is also named Kriging from its original use in geostatistics (Matheron, 1963).

Let  $\mathbf{v}_{\text{pred}} := (\mathbf{x}_{\text{pred}}, \mathbf{t}_{\text{pred}})$  be an input vector (of size  $N \times 1$ ) and  $\mathbf{c}(\mathbf{v}_{\text{pred}}, \mathbf{D}_{\mathbf{N}})$  be the vector of correlations of  $\mathbf{v}_{\text{pred}}$  with  $\mathbf{D}_{\mathbf{N}}$ . The *posterior* distribution of  $Y$  conditional on the simulations  $\mathbf{y}(\mathbf{D}_{\mathbf{N}})$  is Gaussian and can be computed using the formula for the conditional distribution of the multivariate normal distribution:

$$Y^N := Y|\mathbf{y}(\mathbf{D}_{\mathbf{N}}) \sim \mathcal{PG}(\mu_{\beta}^N(\cdot), V_{\Psi}^N), \quad (11)$$

where

$$\mu_{\beta}^N(\mathbf{v}_{\text{pred}}) = \mathbb{E}[Y^N(\mathbf{v}_{\text{pred}})] = m_{\beta}(\mathbf{v}_{\text{pred}}) + \mathbf{c}(\mathbf{v}_{\text{pred}}, \mathbf{D}_{\mathbf{N}})^T \Sigma_{\Psi}^{-1} [\mathbf{y}(\mathbf{D}_{\mathbf{N}}) - m_{\beta}(\mathbf{v}_{\text{pred}})], \quad (12)$$

$$V_{\Psi}^N(i, j) = \text{Cov}(\mathbf{v}_{\text{pred}}^i, \mathbf{v}_{\text{pred}}^j) = \sigma^2(\Sigma_{\Psi}(i, j) - c(\mathbf{v}_{\text{pred}}^i, \mathbf{D}_{\mathbf{N}})^T \Sigma_{\Psi}^{-1} c(\mathbf{v}_{\text{pred}}^j, \mathbf{D}_{\mathbf{N}})). \quad (13)$$

The conditional Gaussian process (11) yields a stochastic prediction of the model for any input  $\mathbf{v}_{\text{pred}}$  of the input space  $\mathcal{X} \times \mathcal{T}$ . In the case where  $\mathbf{v}_{\text{pred}}$  belongs to  $\mathbf{D}_{\mathbf{N}}$ ,

$$\mu_{\beta}^N(\mathbf{v}_{\text{pred}}) = y(\mathbf{v}_{\text{pred}}),$$

and

$$\tilde{\sigma}_N^2(\mathbf{v}_{\text{pred}}) = 0,$$

which is expected for such an emulator of a deterministic computer model. For more details about the Gaussian process emulator, refer to Rasmussen and Williams (2006), Santner et al. (2003), Fang et al. (2006). Other more theoretical references dedicated to asymptotic properties are Stein (1999) and Bachoc (2014).

Thus far, the parameters  $\beta$ ,  $\sigma^2$ ,  $\Psi$  have been assumed to be known. In the calibration model, their estimation is done together with  $\theta$  according to a two-step procedure described hereafter.

**Calibration using a Gaussian Process emulator** Let us turn back to the calibration problem (6). By assuming only  $N$  simulations are allocated to be run,  $y_{\theta}(\mathbf{x})$  is modeled by a Gaussian process emulator. Let

- $\mathbf{m}_{\beta}(\mathbf{D}_{\mathbf{N}})$  and  $\Sigma_{\Psi}(\mathbf{D}_{\mathbf{N}})$  be the mean vector and the correlation matrix of the Gaussian process, each evaluated in  $\mathbf{D}_{\mathbf{N}}$ ,
- $\mathbf{m}_{\beta}(\mathbf{X}_{\mathbf{f}}, \theta)$  and  $\Sigma_{\Psi}(\mathbf{X}_{\mathbf{f}}, \theta)$  be the mean vector and the correlation matrix of the Gaussian process, each evaluated in  $(\mathbf{X}_{\mathbf{f}}, \theta) := ((\mathbf{x}_{\mathbf{f}}^1, \theta), \dots, (\mathbf{x}_{\mathbf{f}}^n, \theta))$ ,
- $\Sigma_{\Psi}(\mathbf{D}_{\mathbf{N}}, (\mathbf{X}_{\mathbf{f}}, \theta))$  be the correlation matrix between  $\mathbf{D}_{\mathbf{N}}$  and  $(\mathbf{X}_{\mathbf{f}}, \theta)$ .

Then, the *posterior* distribution (6) should be replaced by the full integrated likelihood of the data  $\mathbf{d} := (\mathbf{z}_{\mathbf{f}}, \mathbf{y}(\mathbf{D}_{\mathbf{N}}))$  denoted hereafter by  $L^F$ :

$$L^F(\mathbf{d}|\theta, \lambda^2, \sigma^2, \beta, \Psi, \mathbf{D}_{\mathbf{N}}, \mathbf{X}_{\mathbf{f}}) = \int_Y \Pi(\mathbf{d}|\lambda^2, Y) \Pi(Y|\mathbf{X}_{\mathbf{f}}, \mathbf{D}_{\mathbf{N}}, \theta, \sigma^2, \beta, \Psi) dY, \quad (14)$$

where

$$\mathbf{d}|\lambda^2, Y \sim \mathcal{N}\left(Y, \begin{pmatrix} 0 & 0 \\ 0 & \lambda^2 \mathbf{I}_n \end{pmatrix}\right) \quad (15)$$

and

$$Y|\mathbf{X}_f, \mathbf{D}_N, \boldsymbol{\theta}, \sigma^2, \boldsymbol{\beta}, \boldsymbol{\Psi} \sim \mathcal{N}\left(\begin{pmatrix} \mathbf{m}(\mathbf{D}_N) \\ \mathbf{m}(\mathbf{X}_f) \end{pmatrix}, \sigma^2 \begin{pmatrix} \Sigma_{\boldsymbol{\Psi}}(\mathbf{D}_N) & \Sigma_{\boldsymbol{\Psi}}(\mathbf{D}_N, (\mathbf{X}_f, \boldsymbol{\theta})) \\ \Sigma_{\boldsymbol{\Psi}}(\mathbf{D}_N, (\mathbf{X}_f, \boldsymbol{\theta})) & \Sigma_{\boldsymbol{\Psi}}(\mathbf{X}_f, \boldsymbol{\theta}) \end{pmatrix}\right). \quad (16)$$

By knowing that the product of two Gaussian densities is proportional to a Gaussian density, one can prove that

$$L^F(\mathbf{d}|\boldsymbol{\theta}, \lambda^2, \sigma^2, \boldsymbol{\beta}, \boldsymbol{\Psi}, D_N, \mathbf{X}_f) \propto |C_{\boldsymbol{\Psi}}|^{-1/2} \exp -\frac{1}{2} \left[ (\mathbf{d} - (\mathbf{m}(\mathbf{D}_N), \mathbf{m}_{\boldsymbol{\beta}}(\mathbf{X}_f, \boldsymbol{\theta})))^T C_{\boldsymbol{\Psi}}^{-1} (\mathbf{d} - (\mathbf{m}(\mathbf{D}_N), \mathbf{m}_{\boldsymbol{\beta}}(\mathbf{X}_f, \boldsymbol{\theta}))) \right], \quad (17)$$

where

$$C_{\boldsymbol{\Psi}} = \sigma^2 \begin{pmatrix} \Sigma_{\boldsymbol{\Psi}}(\mathbf{D}_N) & \Sigma_{\boldsymbol{\Psi}}(\mathbf{D}_N, (\mathbf{X}_f, \boldsymbol{\theta})) \\ \Sigma_{\boldsymbol{\Psi}}(\mathbf{D}_N, (\mathbf{X}_f, \boldsymbol{\theta})) & \Sigma_{\boldsymbol{\Psi}}(\mathbf{X}_f, \boldsymbol{\theta}) + \frac{\lambda^2}{\sigma^2} \mathbf{I}_n \end{pmatrix}.$$

In practice, the parameters  $\sigma^2$ ,  $\boldsymbol{\beta}$  and  $\boldsymbol{\Psi}$  are unknown and should thus be estimated together with  $\boldsymbol{\theta}$ . But computing good estimators for the parameters using (17) is a difficult problem (Cox et al., 2001). In practice, it is recommended to separate the estimation of the parameters  $(\sigma^2, \boldsymbol{\beta}, \boldsymbol{\Psi})$  from the calibration parameter  $\boldsymbol{\theta}$  because they are of different natures. Hence, the parameters of the Gaussian process are first estimated by maximizing the marginal density of  $\mathbf{y}(\mathbf{D}_N)$  denoted by  $L^M$ :

$$L^M(Y|\sigma, \boldsymbol{\beta}, \boldsymbol{\Psi}, \mathbf{D}_N) \propto \frac{|\Sigma_{\boldsymbol{\Psi}}|^{-1/2}}{\sigma^N} \exp -\frac{1}{2\sigma^2} \left[ (\mathbf{y}(\mathbf{D}_N) - \mathbf{m}(\mathbf{D}_N))^T \Sigma_{\boldsymbol{\Psi}}(\mathbf{D}_N)^{-1} (\mathbf{y}(\mathbf{D}_N) - \mathbf{m}(\mathbf{D}_N)) \right], \quad (18)$$

and then point-estimators  $(\hat{\sigma}^2, \hat{\boldsymbol{\beta}}, \hat{\boldsymbol{\Psi}})$  of  $(\sigma^2, \boldsymbol{\beta}, \boldsymbol{\Psi})$  are plugged into the conditional integrated likelihood denoted hereafter by  $L^C$ :

$$L^C(\mathbf{z}_f|\boldsymbol{\theta}, y(\mathbf{D}_N)) = \int_Y L^C(\mathbf{z}_f|\lambda, Y) \Pi(Y|\mathbf{y}(\mathbf{D}_N), \mathbf{X}_f, D_N, \boldsymbol{\theta}, \hat{\sigma}^2, \hat{\boldsymbol{\beta}}, \hat{\boldsymbol{\Psi}}) dY. \quad (19)$$

In the same way as before, one can prove that

$$L^C(\mathbf{z}_f|\boldsymbol{\theta}, y(\mathbf{D}_N)) \propto |V_{\boldsymbol{\Psi}} + \lambda^2 \mathbf{I}|^{-1/2} \exp -\frac{1}{2} \left[ \mathbf{z}_f - \boldsymbol{\mu}_{\boldsymbol{\beta}}^N(\mathbf{X}_f, \boldsymbol{\theta})^T (V_{\boldsymbol{\Psi}} + \lambda^2 \mathbf{I}_n)^{-1} (\mathbf{z}_f - \boldsymbol{\mu}_{\boldsymbol{\beta}}^N(\mathbf{X}_f, \boldsymbol{\theta})) \right] \quad (20)$$

where

$$\boldsymbol{\mu}_{\boldsymbol{\beta}}^N(\mathbf{X}_f, \boldsymbol{\theta}) := (\boldsymbol{\mu}_{\boldsymbol{\beta}}(\mathbf{x}_f^1, \boldsymbol{\theta}), \dots, \boldsymbol{\mu}_{\boldsymbol{\beta}}(\mathbf{x}_f^n, \boldsymbol{\theta})),$$

is the conditional mean vector of the Gaussian process in  $\mathbf{X}_f$ . In the following, the likelihood (20) is named as the approximated likelihood. It is Gaussian where the vector of unknown simulations  $y_{\boldsymbol{\theta}}(\mathbf{X}_f)$  is replaced by the vector of *posterior* means  $\boldsymbol{\mu}_{\boldsymbol{\beta}}^N(\mathbf{X}_f, \boldsymbol{\theta})$ . Its uncertainty is

assessed by the conditional covariance matrix  $V_{\Psi}$ , adding to  $\lambda^2 \mathbf{I}_n$  in (20). Let  $\Pi^C$  denote the approximated *posterior* distribution induced by (20). Then,

$$\Pi^C(\boldsymbol{\theta}|\mathbf{z}_f, \mathbf{D}_N) \propto L^C(\mathbf{z}_f|\boldsymbol{\theta}, \mathbf{D}_N)\Pi(\boldsymbol{\theta}). \quad (21)$$

An MCMC algorithm can now be performed based on this cheap *posterior* distribution instead of on the target *posterior* distribution (6). The *plug-in* estimation of the parameters is used to limit the complexity of the calculation. However, by encoding a conjugate gamma-normal *prior* distribution on  $(\beta, \sigma^2)$ , the *posterior* distribution of the emulator

$$Y|\mathbf{y}(\mathbf{D}_N), \mathbf{X}_f, D_N, \boldsymbol{\theta}, \sigma^2, \beta, \hat{\Psi}$$

follows a Student distribution (Santner et al., 2003). Unfortunately, (19) has no closed-form expression. Therefore, for the sake of simplicity we will prefer plug-in estimates in the following.

**The design of experiments  $\mathbf{D}_N$**  Thanks to the consistency of the Gaussian process emulator (Vazquez and Bect, 2010b), the larger the number of points in  $\mathbf{D}_N$ , the closer the approximated likelihood  $L^C(\boldsymbol{\theta}|\mathbf{z}_f)$  to  $L(\boldsymbol{\theta}|\mathbf{z}_f)$ . Then,

$$\text{KL}(\Pi^C(\boldsymbol{\theta}|\mathbf{z}_f, \mathbf{D}_N)||\Pi(\boldsymbol{\theta}|\mathbf{z}_f)) \xrightarrow[N \rightarrow \infty]{} 0, \quad (22)$$

where KL denotes the Kullback-Leibler divergence which can measure how far a probability distribution is from another. For theoretical reasons (Cover and Thomas, 2006), it is a relevant choice of a discrepancy between two probability distributions.

Equation (22) makes the calibration based on (21) be consistent. However, when  $N$  is small, the Gaussian process emulator may not efficiently predict the model with precision for some inputs  $(\mathbf{x}, \boldsymbol{\theta})$  where  $\Pi(\boldsymbol{\theta}|\mathbf{z}_f)$  is high. In such a case, the approximated *posterior* distribution  $\Pi^C(\boldsymbol{\theta}|\mathbf{z}_f, \mathbf{D}_N)$  may be very far from the target *posterior* distribution  $\Pi(\boldsymbol{\theta}|\mathbf{z}_f)$ . Although some indicators have been proposed to assess the predictive capability of the emulator (Bastos and O’Hagan, 2008), the calibration error  $\text{KL}(\Pi^C(\boldsymbol{\theta}|\mathbf{z}_f, \mathbf{D}_N)||\Pi(\boldsymbol{\theta}|\mathbf{z}_f))$  cannot be related to them. Most of the time,  $\mathbf{D}_N$  is built as a fixed one stage Space-Filling Design such as *maximin* Latin Hypercube Design (LHD) (Morris and Mitchell, 1995) or *low discrepancy* LHD (Fang et al., 2006; Damblin et al., 2013). In the next section, new algorithms are proposed to build  $\mathbf{D}_N$  sequentially in order to minimize  $\text{KL}(\Pi^C(\boldsymbol{\theta}|\mathbf{z}_f, \mathbf{D}_N)||\Pi(\boldsymbol{\theta}|\mathbf{z}_f))$ .

Let  $SS^N(\mathbf{t})$  be the sum of squares of the residuals calculated by means of the Gaussian process emulator (11). Hence,  $SS^N(\mathbf{t})$  is a random variable. In the case where all inputs  $\{(\mathbf{x}_f^i, \mathbf{t})\}_{1 \leq i \leq n}$  are in  $\mathbf{D}_N$ , then  $\mathbb{E}[SS^N(\mathbf{t})] = SS(\mathbf{t})$  and  $\mathbb{V}[SS^N(\mathbf{t})] = 0$ .

### 3 Adaptive designs for calibration

**The Expected Improvement (EI) criterion** This is used to build adaptive numerical designs for minimizing (or maximizing) a costly black box model  $y$ . After an initial set of  $k$  simulations  $y(\mathbf{D}_k)$  has been run, the EI criterion can assess the expected improvement of a new run in terms of getting close to the unknown global minimum of  $y$ . Let  $\mathbf{v}_{k+1}$  be the input where the EI value is at its highest, meaning that,

$$\begin{aligned} \mathbf{v}_{k+1} &= \operatorname{argmax}_{\mathbf{v}} EI^k(\mathbf{v}), \\ &= \operatorname{argmax}_{\mathbf{v}} \mathbb{E}[(m_k - Y^k(\mathbf{v}))\mathbf{1}_{Y^k(\mathbf{v}) < m_k}], \end{aligned}$$

where  $Y^k$  is the current Gaussian emulator which is built from  $\mathbf{D}_k$ , and

$$m_k = \min \{y(\mathbf{v}_1), \dots, y(\mathbf{v}_{k-1}), y(\mathbf{v}_k)\}$$

is the current minimum of the model. If  $Y^k$  were a deterministic emulator such as the mean  $\mu$  of the Gaussian process, this criterion would be just the difference  $m_k - \mu$  if  $\mu < m_k$  and 0 if  $\mu > m_k$ , which is an intuitive measure of improvement. The algorithm that consists of running the model at the input  $\mathbf{v}_{k+1}$  then updating the emulator from it and starting again is named EGO (*Efficient Global Optimization*) (Jones et al., 1998). Its convergence to the global minimum of  $y$  has been proven under some assumptions about both the regularity of the model and the kernel choice of the Gaussian process  $Y^k$  (Vazquez and Bect, 2010a). In current use, the algorithm is stopped when the number of allocated simulations is over (here  $N$ ) or when the improvement of  $m_k$  becomes negligible. In terms of computational cost, EGO yields better performances than do other methods dedicated to the optimization of black box functions (Ginsbourger, 2009).

Our contribution consists in rewriting the EI criterion with respect to the calibration goal. We apply it to the sum of squares of the residuals (7):

$$EI^k(\boldsymbol{\theta}) = \mathbb{E} \left[ (m_k - SS^k(\boldsymbol{\theta})) \mathbf{1}_{SS^k(\boldsymbol{\theta}) \leq m_k} \right] \in [0, m_k], \quad (23)$$

where  $m_k := \min \{SS(\boldsymbol{\theta}_1), \dots, SS(\boldsymbol{\theta}_{k-1}), SS(\boldsymbol{\theta}_k)\}$ . Let  $\boldsymbol{\theta}^*$  be defined as

$$\boldsymbol{\theta}^* = \underset{\boldsymbol{\theta}}{\operatorname{argmax}} EI^k(\boldsymbol{\theta}). \quad (24)$$

The expectation in Equation (23) is taken with respect to the multivariate Gaussian distribution induced by the distribution of the Gaussian emulator. The EI criterion is therefore applied to a quadratic truncated function of  $Y$ . Another way would have been to approximate  $SS(\boldsymbol{\theta})$  using a Gaussian process emulator as a function of  $\boldsymbol{\theta}$ . By following this idea,  $m_k$  would have updated as  $m_k := \min \{m_k, SS(\boldsymbol{\theta})\}$  forcing  $n$  simulations to be run at each iteration, which is not relevant for large values of  $n$  (see Section 4).

We now aim at reducing the part of calibration uncertainty induced by the sampling of the approximated *posterior* (21) instead of the target *posterior* (6). From the likelihood expression (6), one can see that the goodness-of-fit of the emulator to the computer model is mainly important for the inputs  $(\mathbf{x}_f^i, \boldsymbol{\theta})$  where  $\mathbf{x}_f^i$  is an input of field data belonging to the set  $\{\mathbf{x}_f^1, \dots, \mathbf{x}_f^n\}$  and  $\boldsymbol{\theta}$  is a value of the parameter having a non-negligible *posterior* probability. Unless the prior distribution is totally inconsistent with the field data, the lower the sum of squared residuals  $SS(\boldsymbol{\theta})$ , the higher the likelihood  $L(\mathbf{z}_f|\boldsymbol{\theta})$  and the higher the *posterior* distribution  $\Pi(\boldsymbol{\theta}|\mathbf{z}_f)$ . Inspired from this idea of reducing the uncertainty of the Gaussian process for input factors  $(\mathbf{x}_f^i, \boldsymbol{\theta})$  where  $SS(\boldsymbol{\theta})$  has small values, two new EGO algorithms for building adaptive designs are presented.

**EGO algorithms** The first algorithm corresponds to the exact EGO algorithm based on Equation (23). The second one is more flexible and should be performed when the number of field data  $n$  is larger.

---

Algorithm 1

---

### Initialization

- Build a Space-Filling LHD  $\mathbf{D}_0 \subset \mathcal{X} \times \mathcal{T}$  of size  $N_0$ .
- Run the model over  $\mathbf{D}_0$ .
- Compute  $\hat{\boldsymbol{\theta}}_1$  as the maximum of  $\Pi^C(\boldsymbol{\theta}|\mathbf{z}_f, \mathbf{D}_0)$ .
- $\mathbf{D}_1 = \mathbf{D}_0 \cup \{(\mathbf{x}_f^i, \hat{\boldsymbol{\theta}}_1)\}_{1 \leq i \leq n}$ .
- Update the Gaussian process distribution after running the model over  $\mathbf{D}_1$ .
- Set  $m_1 := SS(\hat{\boldsymbol{\theta}}_1)$ .

**From  $k = 1$ , repeat the following steps as long as  $N_0 + n \times (k + 1) \leq N$ .**

**Step 1**  $\hat{\boldsymbol{\theta}}_{k+1} = \operatorname{argmax}_{\boldsymbol{\theta}} EI^k(\boldsymbol{\theta})$ .

**Step 2** Run the model over all inputs  $\{(\mathbf{x}_f^i, \hat{\boldsymbol{\theta}}_{k+1})\}_{1 \leq i \leq n}$ .

**Step 3**  $\mathbf{D}_{k+1} = \mathbf{D}_k \cup \{(\mathbf{x}_f^i, \hat{\boldsymbol{\theta}}_{k+1})\}_{1 \leq i \leq n}$ .

**Step 4** Update the Gaussian process distribution over  $\mathbf{D}_{k+1}$ .

**Step 5** Let  $m_{k+1} := \min \{m_0, \dots, m_k, SS(\hat{\boldsymbol{\theta}}_{k+1})\}$ .

As the distribution of the Gaussian process emulator is updated, the hyper-parameters  $(\boldsymbol{\beta}, \sigma, \boldsymbol{\Psi})$  are re-estimated. Algorithm 1 is well-suited when the computer model is run on multiple processors. However, running a subset of simulations would be relevant in the case where the number of available processors is lower than  $n$ . For this reason, Algorithm 2 is presented hereafter as a one-at-a-time strategy where only a new single simulation  $\mathbf{x}^* \in \mathbf{X}_f$  is run at each iteration  $\hat{\boldsymbol{\theta}}_k$ . The current minimum  $m_k$  then becomes a random variable, the probability distribution of which is computed from the distribution of the current Gaussian process emulator  $Y^k$ .

#### Algorithm 2

Initialization is similar to Algorithm 1 except that  $\mathbf{D}_1 = \mathbf{D}_0 \cup \{(\mathbf{x}^*, \hat{\boldsymbol{\theta}}_1)\}_{1 \leq i \leq n}$ .

**For  $k = 1, \dots, N - N_0$ , repeat the same steps as in Algorithm 1 except that Step 2 is replaced with Step  $\tilde{2}$  and Step 5 is replaced with Step  $\tilde{5}$ .**

**Step  $\tilde{2}$**  Run the model in  $(\mathbf{x}^*, \hat{\boldsymbol{\theta}}_{k+1})$  where  $\mathbf{x}^* = \max_{\mathbf{x}_f^i \in \mathbf{X}_f} \operatorname{Crit}(\mathbf{x}_f^i, \hat{\boldsymbol{\theta}}_{k+1})$  (see Equations (25) and (27) below).

**Step  $\tilde{5}$**   $m_{k+1} := \min \{\mathbb{E}[SS^k(\hat{\boldsymbol{\theta}}_1)], \dots, m_k, \mathbb{E}[SS^k(\hat{\boldsymbol{\theta}}_{k+1})]\}$

Algorithm 2 should thus be understood as being an approximation of Algorithm 1 where  $m_k$  is the mean of the random variable  $SS^k(\cdot)$  which encodes the uncertainty on the current minimum. In order to reduce the uncertainty of the Gaussian process emulator, a first criterion

may be to run the model at the input  $(\mathbf{x}^*, \hat{\boldsymbol{\theta}}_{k+1})$  where the variance of the emulator is the highest, such that

$$\mathbf{x}^* = \max_{\mathbf{x}_f^i \in \mathbf{X}_f} \mathbb{V}[Y^k(\mathbf{x}_f^i, \hat{\boldsymbol{\theta}}_{k+1})]. \quad (25)$$

Indeed, when the variance of the Gaussian process decreases, the approximated *posterior* distribution (21) comes close to the target *posterior* distribution (6), but the convergence speed remains unknown. A better way might perhaps consist in targeting such a reduction in the emulator uncertainty where the model output is highly variable over  $\theta$  so that a trade-off with the calibration goal is made. The normalized version of such a criterion is thus written as:

$$\mathbf{x}^* = \max_{\mathbf{x}_f^i \in \mathbf{X}_f} \left( \frac{\mathbb{V}(Y^k(\mathbf{x}_f^i, \hat{\boldsymbol{\theta}}_{k+1}))}{\max_{i=1, \dots, n} \mathbb{V}(Y^k(\mathbf{x}_f^i, \hat{\boldsymbol{\theta}}_{k+1}))} \times \frac{\mathbb{V}[y(\mathbf{x}_f^i, \mathcal{T})]}{\max_{i=1, \dots, n} \mathbb{V}[y(\mathbf{x}_f^i, \mathcal{T})]} \right), \quad (26)$$

where  $y(\mathbf{x}_f^i, \mathcal{T}) \in \mathbb{R}$  denotes the image of the subset  $(\mathbf{x}_f^i, \mathcal{T}) \subset \mathcal{X} \times \mathcal{T}$  and  $\mathbb{V}[y(\mathbf{x}_f^i, \mathcal{T})]$  denotes the variance of the random variable  $y(\mathbf{x}_f^i, \mathcal{T})$  with respect to the uniform distribution on  $\mathcal{T}$ . As the model is unknown, an approximation of (26) is computed based on the current Gaussian emulator  $Y^k$ :

$$\mathbf{x}^* = \max_{\mathbf{x}_f^i \in \mathbf{X}_f} \left( \frac{\mathbb{V}(Y^k(\mathbf{x}_f^i, \hat{\boldsymbol{\theta}}_{k+1}))}{\max_{i=1, \dots, n} \mathbb{V}(Y^k(\mathbf{x}_f^i, \hat{\boldsymbol{\theta}}_{k+1}))} \times \frac{\mathbb{V}[\mu_\beta^k(\mathbf{x}_f^i, \mathcal{T})]}{\max_{i=1, \dots, n} \mathbb{V}[\mu_\beta^k(\mathbf{x}_f^i, \mathcal{T})]} \right). \quad (27)$$

Both Algorithms 1 and 2 are new strategies for building adaptive designs oriented to model calibration. The first criterion (25) is proposed to improve the quality of the emulator whereas Criterion (27) is a trade-off with the calibration goal. A typical problem inherent to sequential Kriging is when two experiments come close, making the covariance matrix numerically singular and thus difficult to invert. This matter can arise when both  $\hat{\boldsymbol{\theta}}_k$  is too close to a previous iteration  $\hat{\boldsymbol{\theta}}_{k'}$ , and  $x^*$  is quite the same for both iterations  $k$  and  $k'$ . The usual way to address this issue consists in adding a small diagonal matrix, named the nugget effect, to the covariance matrix.

At Step 4, hyper-parameters for the emulator are re-estimated as done in the seminal EGO work (Jones et al., 1998).

**Computation of the criterion** The EI criterion needs to be computed. By expanding Equation (23), we have :

$$EI^k(\boldsymbol{\theta}) = m_k \left[ \mathbb{P}[SS^k(\boldsymbol{\theta}) < m_k] - \frac{\mathbb{E}[SS^k(\boldsymbol{\theta}) \mathbf{1}_{SS^k(\boldsymbol{\theta}) \leq m_k}]}{m_k} \right] > 0, \quad (28)$$

implying

$$\mathbb{E}[SS^k(\boldsymbol{\theta}) \mathbf{1}_{SS^k(\boldsymbol{\theta}) \leq m_k}] \leq m_k \mathbb{P}[SS^k(\boldsymbol{\theta}) < m_k]. \quad (29)$$

The expression of  $EI^k(\boldsymbol{\theta})$  is based on the probability of a multivariate Gaussian distribution being sampled inside the hypersphere  $B(0, \sqrt{m_k})$ . An expression of  $\mathbb{P}[SS^k(\boldsymbol{\theta}) < m_k]$  can be computed based on its decomposition as an infinite series in central chi-square distribution (Sheil and Muirheartaigh, 1977). However, no closed form exists for computing  $\mathbb{E}[SS^k(\boldsymbol{\theta}) \mathbf{1}_{SS^k(\boldsymbol{\theta}) \leq m_k}]$  (except in the trivial case  $n = 1$ ). Thus, methods like crude Monte Carlo sampling or alternative numerical strategies need to be performed (Genz and Bretz, 2009; Ellis and R., 2007). The

maximum  $\hat{\theta}$  is taken as the value which maximizes  $EI(\theta)$  over a design  $G$ . In this paper,  $G$  is built as a grid after a discretization of the parameter space  $\Theta$  has been made. In the case where  $\mathbb{P}[SS^k(\theta) < m_k]$  is small, the computation of  $\mathbb{E}[SS(\theta)\mathbf{1}_{SS(\theta) \leq m_k}]$  can be avoided as explained hereafter.

---

Computation of  $EI(\theta)$

---

1. Compute  $\mathbb{P}[\mathbf{z}_f - Y_{\theta}^k \in [-m_k, m_k]^n]$  which is an upper bound of  $\mathbb{P}[SS^k(\theta) \leq m_k]$  for each  $\theta$  of  $G$ .
2. Let  $\tilde{\theta} = \max_G \mathbb{P}[\mathbf{z}_f - Y_{\theta}^k \in [-m_k, m_k]^n]$  be a reference value.
3. Compute  $EI^k(\tilde{\theta})$ .
4. Compute  $EI^k(\theta)$  for the values of the subgrid  $\tilde{G} \subset G$  where

$$EI^k(\tilde{\theta}) \geq \mathbb{P}[\mathbf{z}_f - Y_{\theta}^k \in [-m_k, m_k]^n].$$

5. Let  $\hat{\theta} = \operatorname{argmax}_{\theta \in \tilde{G}} EI^k(\theta)$ .

When

$$EI^k(\tilde{\theta}) \geq \mathbb{P}[\mathbf{z}_f - Y_{\theta}^k \in [-m_k, m_k]^n],$$

there is no need to compute  $EI^k(\theta)$  because  $EI^k(\tilde{\theta}) > EI^k(\theta)$ . However, using this upper bound is only relevant when  $n$  is small because in higher dimensions, the hypercube  $[-m_k, m_k]^n$  has a much larger volume than does the hypersphere.

In our experience, both such a discrete optimization over a grid and Monte Carlo sampling work well. We only aim at finding the area of the input space where the likelihood is high, and hence, the global optimum of  $SS(\theta)$  is not expected to be precisely reached. As shown above, the probability of sampling inside the sphere need not be computed when the mean of  $\mathbf{z}_f - Y_{\theta}^k$  is far from 0.

However, importance sampling techniques can reduce the variance of Monte Carlo estimates. We suggest using a mixture distribution between the uniform distribution over the sphere and the original distribution of  $\mathbf{z}_f - Y_{\theta}^k$ . Its density  $h$  is given by

$$h(v) = \frac{1}{2} \times g(v) + \frac{1}{2} \times \frac{\mathbf{1}_{B(0, m_k)}(v)}{V(B(0, m_k))},$$

where  $g$  is the density of  $\mathbf{z}_f - Y_{\theta}^k$  and  $V(B(0, m_k))$  is the volume of the hypersphere of radius  $m_k$ . In the following section, crude Monte Carlo sampling is performed for convenience.

## 4 Simulations

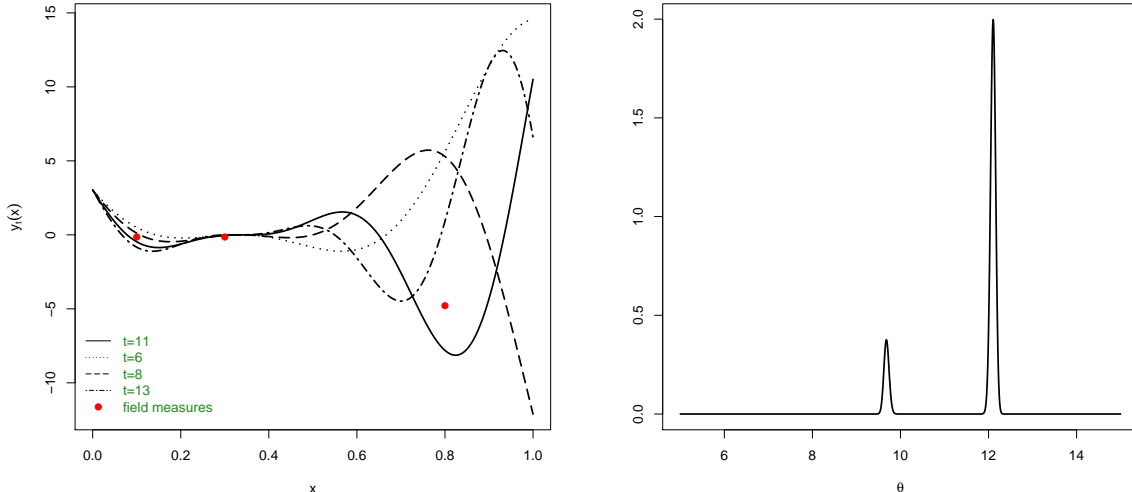
**A 2D example** Let us assume that the computer model is given by the following function:

$$y_t : x \longrightarrow y_t(x) = (6x - 2)^2 \times \sin(tx - 4), \quad (30)$$

where  $x \in \mathcal{X} = [0, 1]$  and  $t \in \mathcal{T} = [5, 15]$ . For  $1 \leq i \leq n$ , the field data  $\mathbf{z}_f$  are generated by

$$z_f^i = y_{\theta}(x_f^i) + \epsilon^i, \quad (31)$$

Figure 1: *Left: the function  $y_t(x) = (6x - 2)^2 \times \sin(tx - 4)$  on  $[0, 1]$  for several values of  $t \in [5, 15]$ . Red dots are the field measures  $(\mathbf{X}_f, \mathbf{z}_f)$  generated by Equation (31). Right: the target posterior distribution.*



where  $\theta = 12$  and  $\epsilon_i \sim \mathcal{N}(0, 0.3^2)$ . Bayesian calibration of (30) is done by sampling the target *posterior* distribution (6) (see Figure 1) where the *prior* distribution  $\Pi(\theta)$  is chosen as uniform on  $[5, 15]$ :

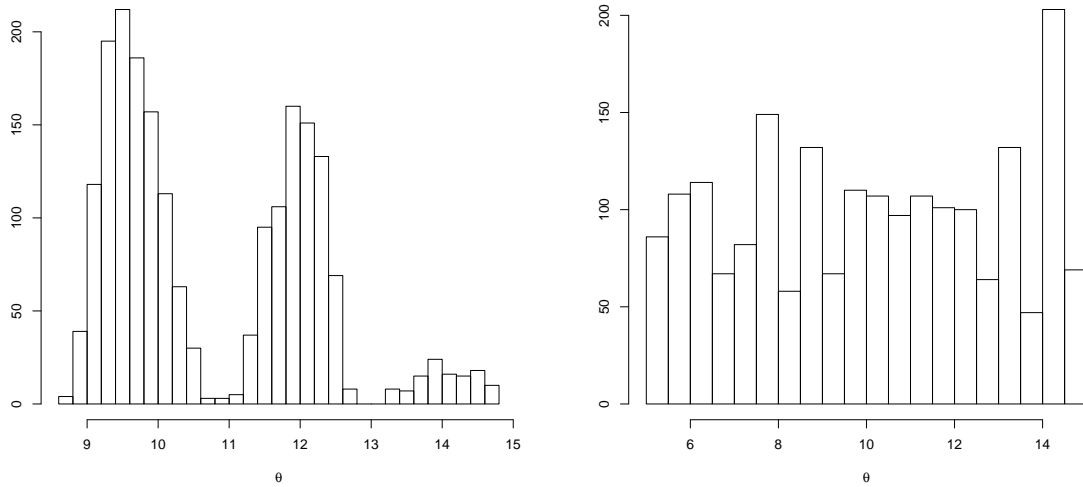
$$\Pi(\theta) \propto \mathbf{1}_{[5, 15]}. \quad (32)$$

Bayesian calibration of Model (30) is done by sampling the approximated *posterior* distribution (21) after choosing a design  $\mathbf{D}_N$ . Comparisons are made to highlight which designs are the most suited in terms of the closeness between the posterior distribution (6) and (21). Two cases are considered: in the first one  $n = 3$ , in the second one  $n = 9$ .

**Case 1:  $\mathbf{X}_f = (0.1, 0.3, 0.8)$**  First, Bayesian calibration of (30) is conducted by sampling the approximated posterior distribution (21) which is built from a maximin LHD of size  $N = 30$ . This calibration is repeated twice by sampling (21) from two different maximin LHD which are built using a simulated annealing routine (implemented in the R library DiceDesign). According to the first one, as illustrated in Figure 2 (left), the regions of high *posterior* density have been clearly identified even though the two modes are reversed in terms of height. According to the second one, as illustrated in Figure 2 (right), the *posterior* distribution is almost flat which leads us to question the capability of the emulator to mimic the function. Such calibrations where the *posterior* distribution is quite far from the target one are unwanted. This example thus raises the question of how many simulations are needed to make the approximated posterior distribution close enough to the target *posterior*. In most cases, without adding information to the model (just taken as a black box function), no clear response can be given to this point, which justifies conducting adaptive calibration. In the following, three new EGO strategies are described:

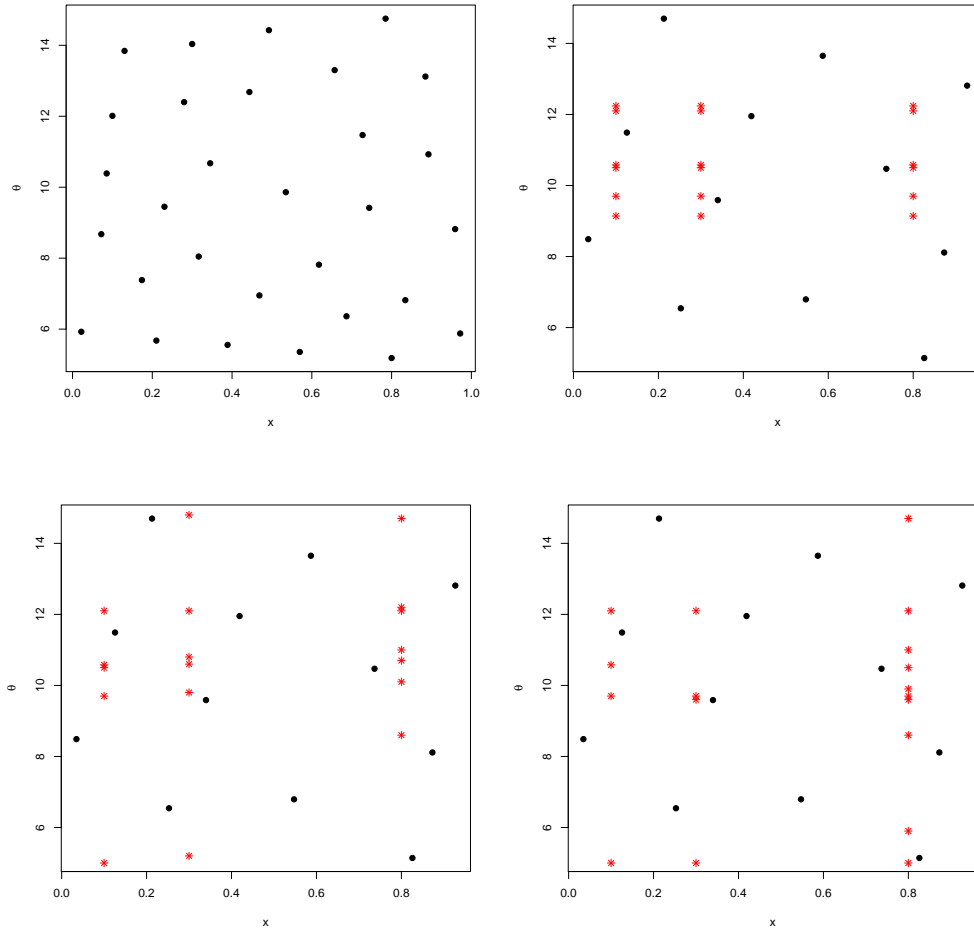
1. a first version based on Algorithm 1. At each iteration, the model is run at all three inputs  $(0.1, \theta_k)$ ,  $(0.3, \theta_k)$ ,  $(0.8, \theta_k)$  where  $\theta_k$  is the current parameter maximizing the EI criterion. An example of a design obtained with this algorithm is displayed in Figure 3 (upper right).

Figure 2: Sampling of (21) from two different maximin LHD (using the R library MCMCpack). The Gaussian process emulator holds a constant mean  $m$  (Ordinary Kriging) and the kernel is the matern  $\frac{5}{2}$ . All parameters  $m, \sigma^2, \Psi$  have been estimated using the R library DiceKriging.



2. a second version based on Algorithm 2. The model is run at a single input  $(x^*, \theta_k)$  where  $x^*$  comes from the input  $(x_i, \theta_k)$  having the highest variance (25) among the three inputs  $(0.1, \theta_k)$ ,  $(0.3, \theta_k)$ ,  $(0.8, \theta_k)$ . An example of a design obtained with this algorithm is displayed in Figure 3 (bottom left).
3. a third version based on Algorithm 2. The model is run at a single input  $(x^*, \theta_k)$  where  $x^*$  comes from the input  $(x_i, \theta_k)$  which maximizes the criterion (27) among the three inputs  $(0.1, \theta_k)$ ,  $(0.3, \theta_k)$ ,  $(0.8, \theta_k)$ . An example of a design obtained with this algorithm is displayed in Figure 3 (bottom right)

Figure 3: Case 1. Upper left: a maximin LHD ( $N = 30$ ). Upper right: a sequential design built from Version 1 ( $N_0 = 12$ ). Bottom left: a sequential design built from Version 2 ( $N_0 = 12$ ). Bottom right: a sequential design built from Version 3 ( $N_0 = 12$ ). The black dots are the initial design. The red stars are the new experiments selected from the EI criterion.



Let us now assess how good the calibration is by computing  $\text{KL}(\Pi^C(\boldsymbol{\theta}|\mathbf{z}_f, \mathbf{D}_N) || \Pi(\boldsymbol{\theta}|\mathbf{z}_f))$  according to the kind of design  $\mathbf{D}_N$  which is used. The proportion of the time that the 95% credibility interval of (21) covers the true value is computed as well. The robustness of the results is checked by repeating sampling of the approximated *posterior* distribution (21) many times. Here, calibration is performed from 50 data sets  $(\mathbf{X}_f, \mathbf{z}_f)$  and for each of them, 50 calibrations derived from 50 different designs have been conducted. In Figure 4, the boxplots of the KL divergence and the boxplots of the coverage are each plotted against the kind of design (including the maximin LHD and the sequential designs coming from the EGO algorithms). Each value of the boxplot is computed as the mean of the criterion over the 50 calibrations derived from a particular data set  $(\mathbf{X}_f, \mathbf{z}_f)$ . A sharp decrease in the KL divergence is noticed when the calibration is done with a sequential design. We can see that both versions 2 and 3 have the lowest values for this criterion. The reason is that Algorithm 2 can move more quickly inside the parameter space  $\mathcal{T}$ , which is expected when the target *posterior* distribution is multimodal. Results about coverage look the same although some lower values can be seen. In such cases,

the coverage is poor because the true value ( $\theta = 12$ ) is not covered by the 95% interval of the target *posterior* distribution. The same feature is thus expected with the approximated *posterior* distribution.

Figure 4: *Case 1. Left: boxplots of the KL divergence computed between the target posterior distribution and the approximated posterior distribution (using the R library FNN). Right: ability of the 95% credibility interval to cover the true value ( $\theta = 12$ ).*

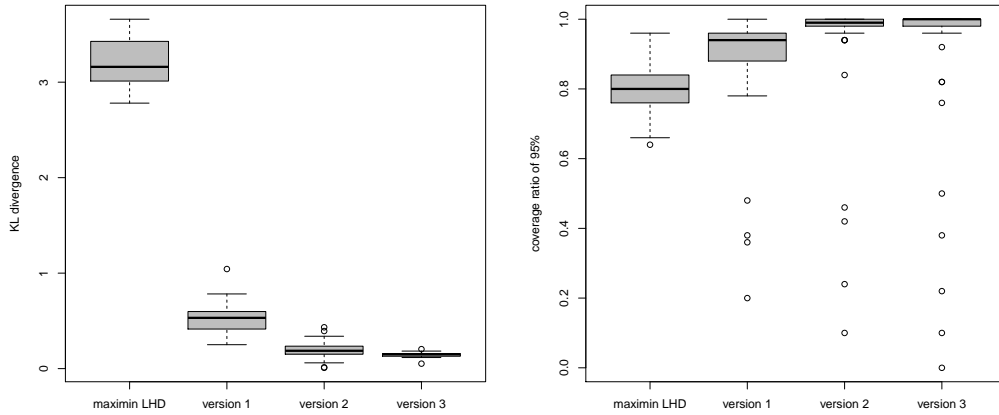
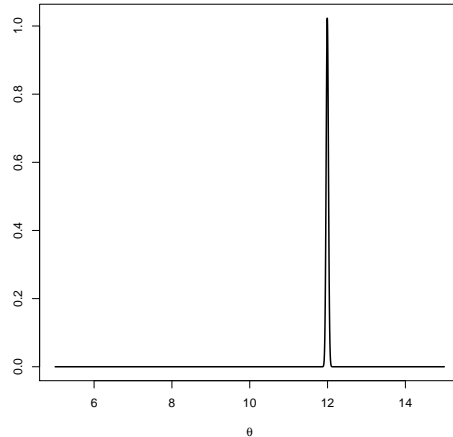


Figure 5: *The target posterior distribution (Case 2)*

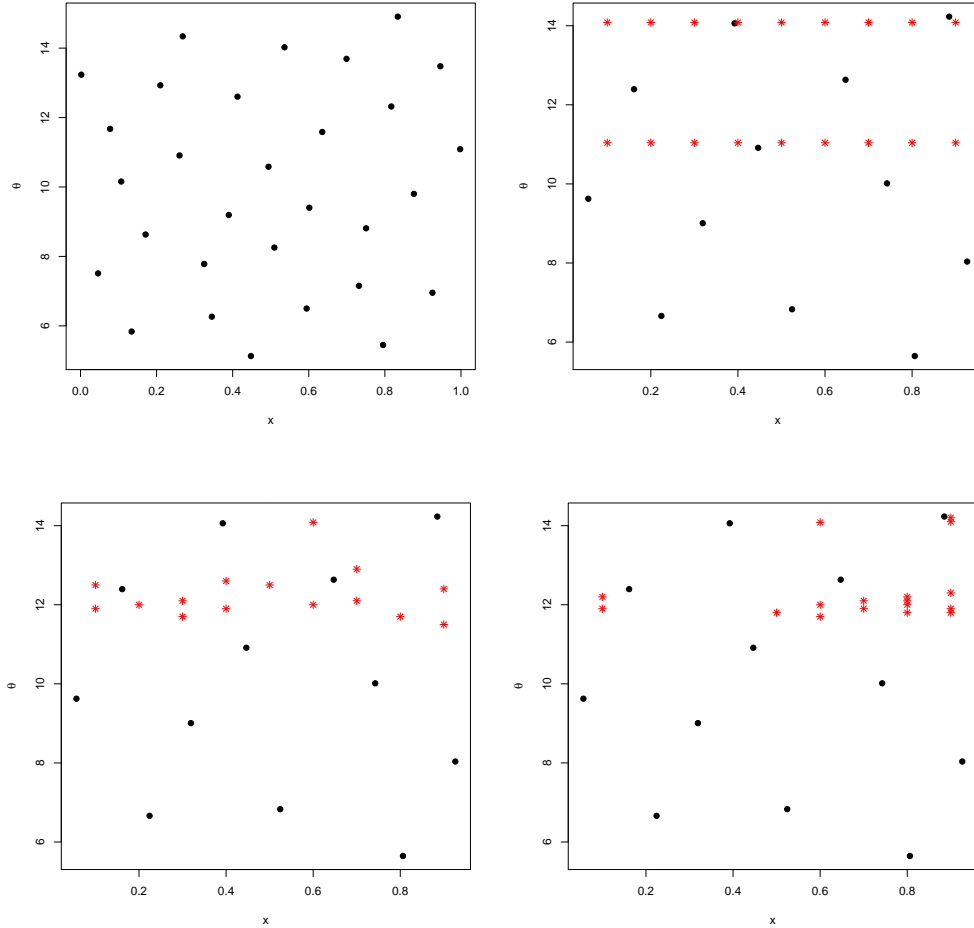


**Case 2:**  $\mathbf{X}_f = (0.1, 0.2, 0.3, 0.4, 0.5, 0.6, 0.7, 0.8, 0.9)$  The field data  $\mathbf{z}_f$  are still generated by

$$z_f^i = y(x_f^i, \theta) + \epsilon^i \quad \text{for } i = 1, \dots, n, \quad (33)$$

where  $\theta = 12$  and  $\epsilon^i \sim \mathcal{N}(0, 0.3^2)$ . As  $n$  is larger, the target *posterior* distribution  $\Pi(\theta|\mathbf{z}_f)$  now has a single narrow mode around the true value. Similar to the first case, the calibration results are improved by using adaptive designs (see Figure 7). As the number of field data is larger, the one-at-a-time Versions 2 and 3 outperform Version 1 because they do not need all

Figure 6: *Case 2. Upper left: a maximin LHD ( $N = 30$ ). Upper right: a sequential design built from Version 1 ( $N_0 = 12$ ). Bottom left: a sequential design built from Version 2 ( $N_0 = 12$ ). Bottom right: a sequential design built from Version 3 ( $N_0 = 12$ ). The black dots are the initial design. The red stars are the new experiments selected from the EI criterion.*



the evaluations corresponding to a  $\theta$  around 14 to discard this area, and evaluations remain to refine the sampling around  $\theta = 12$  (see Figure 6).

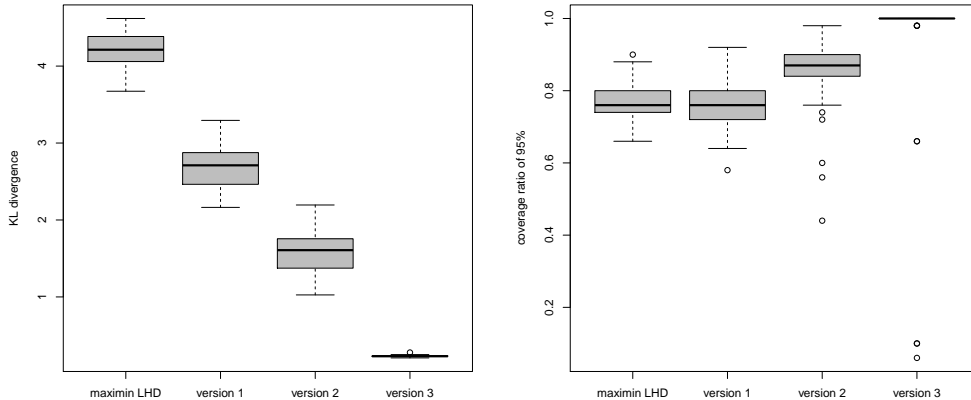
**A 6D example** Inspired from Saltelli et al. (2000), let us now assume that the computer model is given by the following function:

$$g_{\mathbf{t}} : \mathbf{x} \longrightarrow g_{\mathbf{t}}(\mathbf{x}) \prod_{i=1}^3 \frac{|4x_i - 2| + t_i}{1 + t_i}. \quad (34)$$

This highly non-linear function is used within the field of global sensitivity analysis to assess the efficiency of new methods (Marrel, 2008). For  $1 \leq i \leq n = 60$ , the field data  $\mathbf{z}_{\mathbf{f}}$  are still generated by

$$z_f^i = g_{\theta}(x_f^i) + \epsilon^i, \quad (35)$$

Figure 7: *Case 2. Left: boxplots of the KL divergence computed between the target posterior distribution and the approximated posterior distribution (using the R library FNN). Right: ability of the 95% credibility interval to cover the true value ( $\theta = 12$ ).*



where  $\boldsymbol{\theta} = (0.34, 0.34, 0.34)$  and  $\epsilon^i \sim \mathcal{N}(0, 0.05^2)$ . Here, both  $\mathbf{x}$  and  $\boldsymbol{\theta}$  are three-dimensional vectors. In the same spirit as before, we aim at reducing the calibration error between the unknown target *posterior* (6) and the approximated *posterior* (21). The *prior* distribution  $\Pi(\boldsymbol{\theta})$  is chosen as uniform on  $[0, 1]^3$ :

$$\Pi(\boldsymbol{\theta}) \propto \mathbf{1}_{[0,1]^3}. \quad (36)$$

Let the allocated number of simulations be equal to  $N = 200$ . Similar to the 2D example, maximin LHD are compared with the sequential designs. Given the size of field data ( $n = 60$ ), only Version 2 and Version 3 are performed, both starting from an initial design of size  $N_0 = 100$  simulations. As explained in Section 3, a discretization  $G$  of the parameter space is required for maximizing the EI criterion. Given that the dimension of  $\boldsymbol{\theta}$  is larger than in the previous example, the choice of such a grid is more sensitive. Indeed, if  $G$  is too coarse, some promising area of the parameter space may not be explored whereas if  $G$  is too fine, the computation time is drastically increased. The solution that we suggest to address this problem consists in maximizing the EI criterion alternatively on several designs, as iterations, so that:

$$G = G_1 \cap G_2 \cap \dots \cap G_M \quad (37)$$

and

$$G_1 \cap G_2 \cap \dots \cap G_M = \emptyset. \quad (38)$$

In this example, for simplicity we have chosen  $G_1$  and  $G_2$  as two grids where,

$$G_1 = [0, 0.2, 0.4, 0.6, 0.8, 1] \times [0, 0.2, 0.4, 0.6, 0.8, 1] \times [0, 0.2, 0.4, 0.6, 0.8, 1]$$

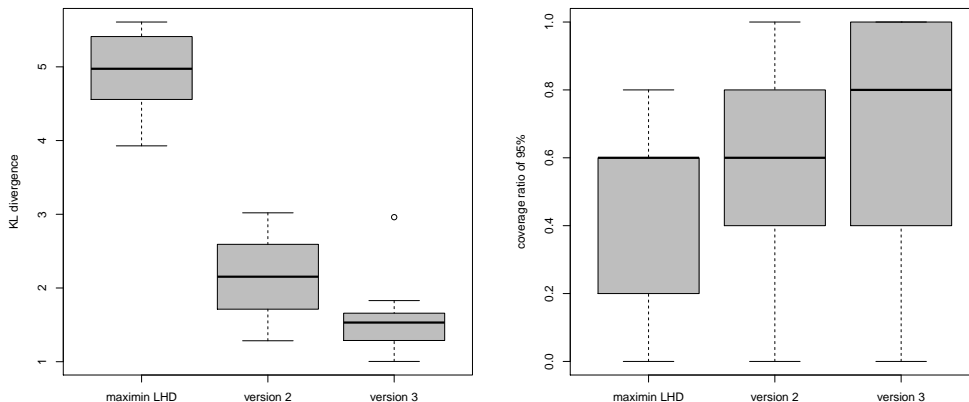
and

$$G_2 = [0.1, 0.3, 0.5, 0.7, 0.9] \times [0.1, 0.3, 0.5, 0.7, 0.9] \times [0.1, 0.3, 0.5, 0.7, 0.9].$$

Thus, for odd iterations the EI criterion is maximized over  $G_1$  whereas for even iterations the EI criterion is maximized over  $G_2$ . The calibration results are illustrated in Figure 8. They look the same as those of the 2D example, which again supports the advantage of using a sequential design. Let us see that neither  $G_1$  nor  $G_2$  covers the unknown true value. One can

think that a more exhaustive decomposition in (37) would make  $G$  closer to the true value  $\theta = (0.34, 0.34, 0.34)$ , perhaps making the results even better. Boxplots for coverage rate have larger variance than in the previous examples because the 95% credibility interval of each marginal distribution needs to cover the true value 0.34.

Figure 8: *Left: boxplots of the KL divergence computed between the target posterior distribution and the approximated posterior distribution (using the R library FNN). Right: Coverage rate. For both figures, boxplots are made over 50 calibrations.*



## 5 Conclusion

This work deals with new adaptive numerical designs for the calibration of non-linear computer models requiring time-consuming simulations. After computing a cheap-to-evaluate *posterior* distribution of the model parameters based on a Gaussian stochastic process of the model, we take advantage of the probability distribution of this emulator for proposing a criterion to optimize in order to make this approximated *posterior* distribution close to the unknown target *posterior* distribution. Such an aim requires reducing the uncertainty of the emulator where the target *posterior* distribution has a high density. As this distribution is unknown, a new strategy is proposed which consists in applying the EI criterion to the sum of squares of the residuals between the available field data and the computer model.

The fact that the *prior* distribution is not taken into account in the EI maximization may appear surprising. Yet the reason is that the *prior* distribution remains the same for both the approximated *posterior* distribution and the target *posterior* distribution. We also argue that the *prior* is not unique and thus one should be capable of performing several calibrations from several different *prior* distributions without starting over an EGO algorithm. In this paper, the algorithms are described in an unbiased framework by assuming that there is no discrepancy between the physical system and the computer model. We also suppose there is no correlation between the residuals. In a case where *prior* information were available for either of these errors, the algorithms could be performed from a weighted sum of squares function in a similar way. The results obtained under the unbiased framework are in favor of using our new designs in the sense that the approximated *posterior* distributions of synthetic functions in 2D and 6D are very close to the target *posterior* distribution.

The main difference between the algorithms introduced in this paper and the current use

of the EGO algorithm is that the sum of squares of the residuals is not itself modeled by a Gaussian process. It is approximated as a stochastic process against  $\theta$  which is computed from the Gaussian process emulator on the model. This modeling makes it possible to carry out one-at-a-time sequential strategies where a single simulation  $y_{\hat{\theta}_k}(\mathbf{x}^*)$  is run at each iteration (see Algorithm 2). Two criteria have been suggested to pick up  $\mathbf{x}^*$  among the input field measures  $\mathbf{X}_f$ . In higher dimensions, other criteria might be more relevant. For example,  $\mathbf{x}^*$  could be chosen inside the region  $\mathcal{X} \times \{\hat{\theta}_k\}$  with the help of the Stepwise Uncertainty Reduction (SUR) strategy (Bect et al., 2012) applied to the variance of the sum of squares of the residuals.

Another concern is how to maximize the EI criterion over the parameter space  $\Theta$ . Because in our framework this criterion has no closed-form expression, making gradient methods unfeasible, the optimization is performed over a numerical design of experiments. The choice of such a design is critical, requiring a trade-off between the computation time and the quality of the optimization, especially if the parameter space  $\Theta$  is high dimensional. Such a question should be the subject of a future work. Finally, our EGO algorithms start from a maximin LHD on  $\mathcal{X} \times \Theta$  while the *posterior* distribution only depends on the simulations running inside the region  $\mathbf{X}_f \times \Theta$ . Another solution would have been to build Space-Filling Designs on such spaces.

## 6 Acknowledgements

The authors of the paper want to thank Joan Sobota for correcting English mistakes.

## References

- Bachoc, F. (2014). Asymptotic analysis of the role of spatial sampling for covariance parameter estimation of Gaussian processes. *Journal of Multivariate Analysis*, 125:1–35.
- Barbillon, P., Celeux, G., Grimaud, A., Lefebvre, Y., and Rocquigny (De), E. (2011). Non linear methods for inverse statistical problems. *Computational Statistics and Data Analysis*, 55:132–142.
- Bastos, L. and O’Hagan, A. (2008). Diagnostics for Gaussian process emulators. *Technometrics*, 51:425–438.
- Bayarri, M., Berger, J., Paulo, R., Sacks, J., Cafeo, J., Cavendish, J., Lin, C., and Tu, J. (2007). A framework for validation of computer models. *Technometrics*, 49:138–154.
- Bect, J., Ginsbourger, D., Li, L., Picheny, V., and Vazquez, E. (2012). Sequential design of computer experiments for the estimation of a probability of failure. *Statistics and Computing*, 22(3):773–793.
- Bernardo, J. M. and Smith, A. F. M. (1994). *Bayesian Theory*. Wiley, London, 1st edition.
- Campbell, K. (2006). Statistical calibrations of computer simulations. *Reliability Engineering and System Safety*, 91:1358–1363.
- Cover, T. and Thomas, J. (2006). *Elements of Information Theory 2nd Edition*. Wiley, New York.
- Cox, D., Park, J., and Clifford, E. (2001). A statistical method for tuning a computer code to a data base. *Computational Statistics and Data Analysis*, 37:77–92.

- Craig, P., Goldstein, M., Seheult, A., and Smith, J. (1997). *Pressure Matching for Hydrocarbon Reservoir History: A Case Study in the Use of Bayes Linear Strategies for Large Computer Experiments*, volume 121 of *Lecture Notes In Statistics*. Springer-Verlag.
- Damblin, G., Couplet, M., and Iooss, B. (2013). Numerical studies of space filling designs: optimization of Latin hypercube samples and subprojection properties. *Journal of simulation*, 7:276–289.
- Ellis, N. and R., M. (2007). Multivariate Gaussian simulation outside arbitrary ellipsoids. *Journal of Computational and Graphical Statistics*, 16:692–708.
- Fang, K., Li, R., and Sudijianto, A. (2006). *Design and modeling for computer experiments*.
- Genz, A. and Bretz, F. (2009). *Computation of Multivariable Normal and t Probabilities*, volume 195 of *Lecture Notes In Statistics*. Springer, New York.
- Ginsbourger, D. (2009). *Multiplés Métamodèles pour l’approximation et l’optimisation de fonctions numériques multivariées*. PhD thesis, Ecole Nationale Supérieure des Mines de Saint-Etienne.
- Higdon, D., Kennedy, M., Cavendish, J., Cafo, J., and Ryne, R. (2004). Combining field data and computer simulations for calibration and prediction. *SIAM Journal on Scientific Computing*, 26:448–466.
- Janusevskis, J. and Le Riche, R. (2013). Simultaneous kriging-based estimation and optimization of mean response. *Journal of Global Optimization*, 55:313–336.
- Jones, D., Schonlau, M., and Welch, W. (1998). Efficient global optimization of expensive black-box functions. *Journal of Global Optimization*, 13:455–492.
- Keller, M., Pasanisi, P., and Parent, E. (2011). Réflexions sur l’analyse d’incertitude dans un contexte industriel: information disponible et enjeux décisionnels. *Journal de la Société Française de Statistique*, 152(4):60–77.
- Kennedy, M. and O’Hagan, A. (2001). Bayesian calibration of computer models (with discussion). *Journal of the Royal Statistical Society, Series B, Methodological*, 63:425–464.
- Koehler, J. and Owen, A. (1996). Computer experiments. *Handbook of Statistics, Vol.13*.
- Kumar, A. (2008). *Sequential calibration of computer models*. PhD thesis, The Ohio State University.
- Loeppky, D., Bingham, D., and Welch, W. (2006). Computer model calibration or tuning in practice. *Technical Report*.
- Marrel, A. (2008). *Mise en oeuvre et utilisation du méta-modèle processus gaussien pour l’analyse de sensibilité de modèles numériques*. PhD thesis, CEA Cadarache.
- Matheron, G. (1963). Principles of geostatistics. *Economic Geology*, 58:1246–1266.
- Morris, D. and Mitchell, J. (1995). Exploratory designs for computational experiments. *Journal of Statistical Planning and Inference*, 43:381–402.

- Parent, E. and Bernier, J. (2007). *Le Raisonnement Bayésien : Modélisation et Inférence*. Springer France, Paris.
- Pratola, M., Sain, S., Bingham, D., Wiltberger, M., and Rigler, E. (2013). Fast sequential computer model calibration of large nonstationary spatial-temporal processes. *Technometrics*, 55:232–242.
- Rasmussen, C. and Williams, C. (2006). *Gaussian Processes for Machine Learning*. the MIT press.
- Robert, C. and Casella, G. (1998). *Monte Carlo Statistical Methods*. Springer-Verlag.
- Roy, C. and Oberkampf, W. (2011). A comprehensive framework for verification, validation and uncertainty quantification in scientific computing. *Computer Methods in Applied Mechanics and Engineering*, 200:2131–2144.
- Saltelli, A., Chan, K., and Scott, E. (2000). *Sensitivity Analysis*. Wiley, New York.
- Santner, T., Williams, B., and Notz, W. (2003). *The Design and Analysis of Computer Experiments*. Springer-Verlag.
- Sheil, J. and Muirheartaigh, I. (1977). The distribution of non-negative quadratic forms in normal variables. *Journal of the Royal Statistical Society*, 26:92–98.
- Stein, M. (1999). *Interpolation of Spatial Data: Some Theory for Kriging*. Springer.
- Trucano, T., Swiler, L., Igusa, T., Oberkampf, W., and Pilch, M. (2006). Calibration, validation and sensitivity analysis: What’s what. *Reliability Engineering and System Safety*, 91:1331–1357.
- Vazquez, E. (2005). *Modélisation comportementale de systèmes non-linéaires multivariés par méthodes à noyaux et applications*. PhD thesis, Université Paris Sud.
- Vazquez, E. and Bect, J. (2010a). Convergence properties of the expected improvement algorithm with fixed mean and covariance functions. *Journal of Statistical Planning and Inference*, 140:3088–3095.
- Vazquez, E. and Bect, J. (2010b). Pointwise consistency of the kriging predictor with known mean and covariance functions. *mODa 9 – Advances in Model-Oriented Design and Analysis Contributions to Statistics*, pages 221–228.
- Williams, B. J., Loepky, J. L., Moore, L. M., and Mason, M. S. (2011). Batch sequential design to achieve predictive maturity with calibrated computer models. *Reliability Engineering and System Safety*, 96:1208–1219.
- Williamson, D. and Vernon, I. (2015). Efficient uniform designs for multi-wave computer experiments. *Journal of the American Statistical Association*.